Organic Electronics 13 (2012) 366–372

Contents lists available at SciVerse ScienceDirect

Organic Electronics

journal homepage: www.elsevier.com/locate/orgel

C_{60}/NiFe combination as a promising platform for molecular spintronics

M. Gobbi [a,*], A. Pascual [a], F. Golmar [a,b], R. Llopis [a], P. Vavassori [a,c], F. Casanova [a,c], L.E. Hueso [a,c]

[a] CIC NanoGUNE Consolider, Tolosa Hiribidea 76, 20018 Donostia–San Sebastian, Basque Country, Spain
[b] I.N.T.I.–CONICET, Av. Gral. Paz 5445 Ed. 42, B1650JKA, San Martín, Bs As, Argentina
[c] IKERBASQUE, Basque Foundation for Science, 48011 Bilbao, Basque Country, Spain

ARTICLE INFO

Article history:
Received 6 October 2011
Received in revised form 30 November 2011
Accepted 1 December 2011
Available online 13 December 2011

Keywords:
Spintronics
Organic electronics
Fullerene
Spin valves
Magnetism
Atomic force microscopy

ABSTRACT

Spintronics based on ferromagnetic metals and organic semiconductors has attracted great interest in recent years. Molecular-based spintronic devices, such as magnetic tunnel junctions, have been demonstrated with performances competing with those of conventional inorganic devices. Still, there is huge margin for improvement, as many details about the injection of spin-polarized electrons into the molecular layer remain not completely understood. In order to achieve better understanding and control of the physical mechanisms, it is necessary to explore various combinations of ferromagnetic metals and organic semiconductors.

In this letter, we study the properties of the combination between the ferromagnetic metal NiFe (commonly known as Permalloy or Py) and the molecular system C_{60}. We produced C_{60}/Py bilayers and characterized them structurally, electrically and magnetically. The C_{60} films grow smoothly on both Py and SiO_2 substrates, and we estimate that a 5-nm-thick C_{60} film covers completely the surface underneath without leaving pinholes and can be therefore used in a vertical device, as confirmed by electrical characterization. Furthermore, the C_{60} film is robust against the deposition of the top metal electrode, being the intermixing layer of only 1–2 nm at the C_{60}/Py interface. Finally, we show that the magnetic properties of Py are not affected by the deposition sequence, and that a 5-nm-thick Py layer on top of a C_{60} layer keeps its magnetic properties intact.

These results show that the combination between Py and C_{60} provides a robust template platform for the development of molecular spintronics, and can be used later on for more sophisticated investigations, such as the role of the interfaces in the spin injection.

1. Introduction

Π-Conjugated organic semiconductors have emerged recently as promising candidates for spintronic applications [1]. Most of the excitement about these materials comes from the fact that they present very weak mechanisms for spin scattering, mainly due to the majoritarian presence of light elements such as carbon, hydrogen and nitrogen.

Indeed, organic spintronic devices have been demonstrated, very often in a vertical spin-valve geometry, in which a molecular layer is sandwiched between two spin-polarized ferromagnetic (FM) metals (see Fig. 1 for a scheme of a typical spin valve). Spin polarized electrons are transported between the FM metals, and a clear difference in the electrical resistance of the device is measured depending on the relative alignment of the FM electrodes magnetization, being this magnetoresistance a proof of spin conservation across the molecular interlayer [2–8].

The performance of different devices, measured typically in terms of their magnetoresistance ratio, depends crucially on both the FM metal and the organic material employed [1] and also on microscopic details of the interface between them [2,9–11]. Several combinations of FM metals and organics have been investigated [12–19], but

* Corresponding author.
E-mail address: m.gobbi@nanogune.eu (M. Gobbi).

1566-1199/$ - see front matter © 2011 Elsevier B.V. All rights reserved.
doi:10.1016/j.orgel.2011.12.002

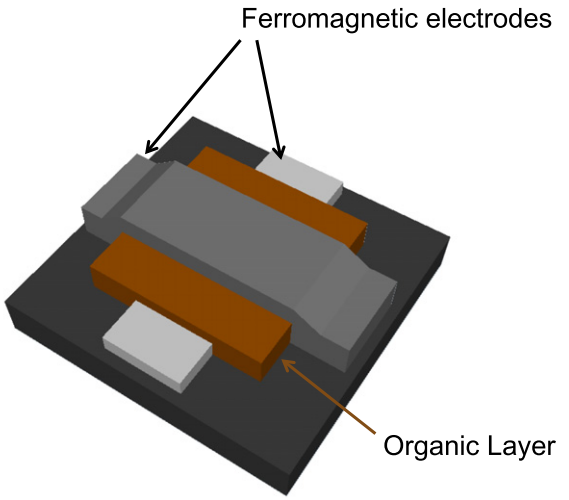

Fig. 1. Scheme of a typical organic spin valve with an organic layer sandwiched between two FM electrodes.

so far it has been challenging to predict the arising electrical performance only on the basis of the interface properties due to the complexity of the mutual interactions between so dissimilar materials.

Therefore, it would be of great importance to find a robust material combination to be used as a reliable template for molecular spintronics. This template would allow later on more sophisticated investigations, such as the role of the interfaces in the spin injection, or the injection of spin polarized electrons in molecules using alternative methods, employing for instance spin-filtering tunnel barriers [20] or ballistic electrons [21].

In this letter we show how the combination of Permalloy (Py; $Fe_{81}Ni_{19}$) and C_{60} fullerene has several magnetic and structural properties that make it a promising test system for molecular spintronics. Permalloy was chosen because it is a well characterized 3d FM metal widely used in spintronic applications [22,23]. It is fairly resistant to oxidation and has a high Curie temperature (T_C = 830 K), making it ideal for devices operating at room temperature. Moreover, it presents a very small magnetic anisotropy (so shape only can be used to engineer the macroscopic magnetic behavior) and a relatively high spin polarization (about 40%).

C_{60} fullerene, one of the known allotropes of carbon with application in electronics, is attracting interest as well in the field of molecular spintronics [5,19,24,25], where C_{60}-based vertical spin-valves have already been reported [5]. In fact, C_{60} has some unique properties making it perfectly suited for spintronic application. First, it is composed by C-atoms only unlike most organic semiconductors that contain H atoms. The hyperfine interaction with H nuclei, which is one of the main sources of spin scattering for organic materials for OS [8], is therefore absent. Second, it can be evaporated in UHV conditions for a clean interfacing with metals. Finally, it is a standard and easily accessible molecule in high purity form, ideal for being employed as a platform for molecular spintronics.

2. Materials and methods

In the current study, Py/C_{60} bilayers were fabricated in situ in a dual chamber UHV evaporator with a base pressure below 10^{-9} mbar. One chamber is dedicated to the Py deposition by means of electron-beam evaporation, while in the second one the C_{60} fullerene is thermally evaporated. High purity materials were employed: Py 99.95% purity (Lesker) and C_{60} 99.9% (Sigma Aldrich). All the samples described were grown on Silicon substrates covered by a thin SiO_2 native layer.

In order characterize the structural and magnetic properties of the metal/fullerene system, we have fabricated two different sets of bilayers. In the first set, we deposited a bottom Py layer, with a fixed thickness of 5 nm, and subsequently a C_{60} layer with variable thickness (from 5 up to 25 nm) on top of it. In the second set, we reversed the deposition sequence and deposited a bottom 16-nm-thick C_{60} layer, covered in this case by a top Py layer with variable thickness (again in the range from 5 up to 25 nm). The samples of this second set were completed with the deposition of a 2 nm Al capping layer to prevent the oxidation of the Py layer.

The structural characterization of the samples was carried out by combining atomic force microscope (AFM) and X-ray reflectivity (XRR) measurements. AFM images were recorded in standard tapping mode with an Agilent microscope. X-ray reflectivity was performed in an X'Pert Panalytical system. The XRR data are analyzed with the software "Panalytical X'Pert Reflectivity", which allows the simulation and the fitting to experimental data of multilayer structures composed of different materials. A layer in the structure is defined by its thickness, density and roughness, which are free as fitting parameters.

Magnetic characterization was performed combining absolute magnetization and magneto-optical hysteresis loops. Magnetization was measured in a Quantum Design VSM-SQUID magnetometer, while magneto-optical data were recorded in a home-made magneto-optical Ker effect (MOKE) apparatus [26].

For the electrical characterization, we produced vertical devices with a 20-nm-thick Py used as a top electrode above a variable-thickness C_{60} layer and a cobalt (Co) bottom electrode. A seed layer of aluminum oxide (AlO_x) was inserted between the Co and the C_{60} layer. Further details on the fabrication of these specific devices are given elsewhere [5]. The electrical characterization was performed in a Lakeshore probe station at room temperature, using a 4-point configuration.

3. Results and discussion

For the growth of vertical spin valves with thin molecular layers sandwiched between two metallic contacts, some constrains need to be fulfilled by both the molecular and the metal layer:

(1) The molecular layer needs to grow smoothly with low surface roughness, covering completely the bottom metal contact after the deposition of a few

monolayers. In this way, the metal film grown on top of the molecular layer would be in contact with the molecules only, without touching directly the metal underneath (pinholes). Furthermore, a low surface roughness is important to achieve homogeneous conductance through the molecular layer, since if the surface is very rough the current will flow mainly through those regions that present the lowest thickness.

(2) The top metal contact should not penetrate deeply in the organic layer during the deposition. Certain intermixing layer at the metal–organic interface is probably unavoidable [27–30], but it should be as thin as possible (in the order of 1 nm).

(3) For being an optimal spin injector, the FM metal layers need to maintain their magnetic properties intact, either when they are deposited at the bottom or at the top of the vertical structure. In this article we show how the Py/C_{60} system fulfills the three conditions listed above, making it a promising testing platform in molecular spintronics.

Starting from the morphological characterization, we summarize the surface information obtained by AFM in Fig. 2. Fig. 2a–c refers to the set of Py/C_{60} samples in which Py is the bottom film and C_{60} the top one.

Fig. 2a shows an AFM micrograph of a single 5-nm-thick nm Py film grown on the Si/SiO_2 substrate. The analysis indicates that the film is a polycrystal formed by flat nano-sized grains with an average lateral grain size (d) of 15 nm. Its surface is extremely smooth, with a rms roughness (r) of 0.19 nm across a 1 × 1 μm image (Fig. 1a). Fig. 2b shows the surface of a Py (5 nm)/C_{60} (3 nm) bilayer. In this case, although the average lateral grain size of the topmost C_{60} surface is also around 15 nm, as for the plain Py film, while the rms roughness is much higher being $r = 0.43$ nm and with a peak-to-peak value in excess of 3 nm (Fig. 2b). Comparing this roughness with the outer diameter of the C_{60} molecule (diameter around 1 nm) we estimate the overall roughness to be about 3–4 molecular layers. The fact that the layer roughness is comparable with the layer thickness suggests that the coverage of the Py surface may be discontinuous. Therefore, such a thin C_{60} layer is not suitable for the growth of a vertical device, as pinholes are very likely to form upon the deposition of a top metal contact. In the samples with thicker C_{60} layers, the lateral grain size slightly increases reaching an average value $d = 25$ nm for the 25-nm-thick film (a direct comparison can be done by inspection of Fig. 2b and c). However, the rms roughness of the C_{60} layer surface does not change significantly with its thickness, as it maintains in the range $r = 0.4$–0.5 nm with peak-to-peak roughness in excess of 3 nm (Fig. 2b and c). Given these rms and peak-to peak roughnesses, we estimate that a 5-nm-thick C_{60} film forms a continuous layer on the metal surface, and hence it could be used as interlayer in a vertical device.

We can turn out now our attention to the topography of the Py films grown over a fullerene underlayer (Fig. 2d–f). A 16-nm-thick C_{60} layer deposited directly on the substrate is shown in Fig. 2d. This layer is formed by grains with an average lateral size of 20 nm, in good agreement with AFM data reported in literature [31]. In this case, the rms roughness is $r = 0.65$ nm, with the peak-to-peak roughness in excess of 3.5 nm. This peak-to-peak roughness shows that the morphology of the surface of the C_{60} layers is substantially independent of the substrate utilized, either SiO_2 or Py. When a Py layer is subsequently grown on top of the 16-nm-thick C_{60} film, its surface morphology mimics that of the C_{60} layer underneath, both in terms of grain size and of surface roughness, irrespectively of the Py thickness. The peak-to-peak roughness value of ~3–3.5 nm sets the limiting thickness required for obtaining a continuous

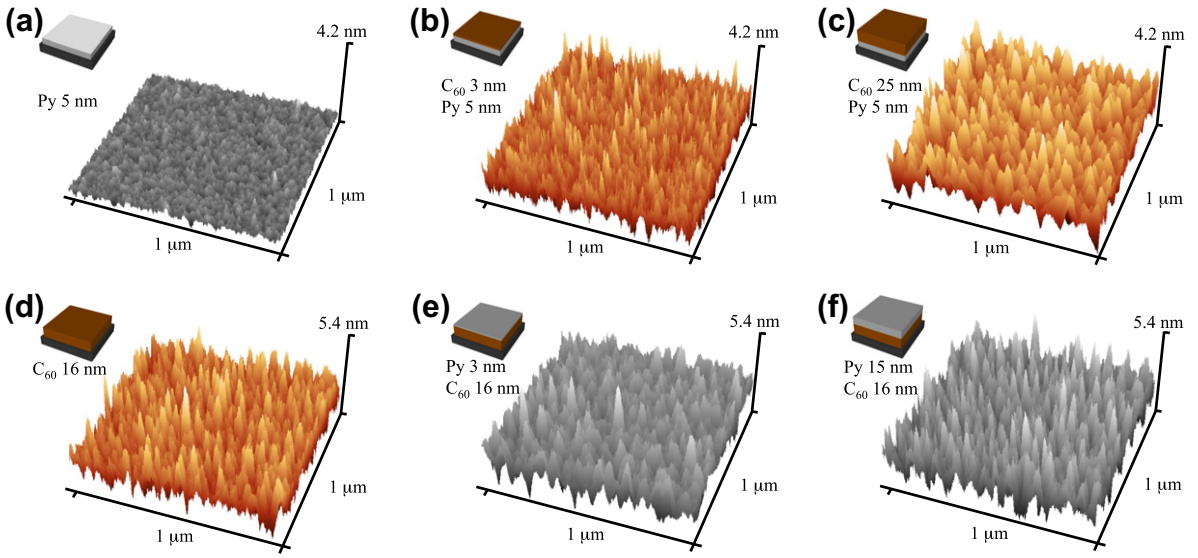

Fig. 2. AFM characterization of Py/C_{60} and C_{60}/Py bilayers. Py surfaces are shown in grey scale, C_{60} surface in brown scale. (a–c) Images of samples Py/C_{60}, Py below C_{60}: (a) surface of a 5 nm Py layer with no top C_{60}; (b) 5 nm Py covered by 3 nm C_{60}; (c) 5 nm Py covered by 25 nm C_{60}. (d–f) Images of samples C_{60}/Py, with C_{60} below Py: (d) surface of 15 nm C_{60} with no top Py; (e) 16 nm C_{60} covered by 3 nm Py; (f) 16 nm C_{60} covered by 15 nm Py.

layer both in the Py and C_{60} case. For the case of a thin Py layer (thickness <4 nm), its discontinuous film structure will be confirmed by the magnetic characterization of the samples (see below).

In addition to AFM, we have also used X-ray reflectivity (XRR) to check the layer thickness and homogeneity on a larger scale (mm^2 compared to μm^2 for the AFM analysis). Interference fringes (also called Kiessig or Laue fringes) are present in XRR scans on both single Py and C_{60} layers of similar thickness (Fig. 3a and b), confirming the high quality of the surfaces under study. In the particular case of a single Py film, the fringes pattern extend up to an angle of 3°, while in a single C_{60} layer they are no longer discernible from the noise background above 1.5°. This fact indicates that the large area roughness of Py is lower than for the C_{60}, in good agreement with the AFM measurements (see above). In particular, from the XRR fittings we extract a large area roughness of $r = 0.4$ nm (for the Py film) and $r = 1.4$ (for the C_{60} film).

Following the overall analysis of both AFM and XRR data, we can conclude that the Py/C_{60} system fulfills the first condition listed above for a material to become a suitable test platform for molecular spintronics.

We move now into condition two of the criteria outlined above. To this purpose, information on the damage caused to the molecular layer by the top metal deposition can be obtained by comparing XRR scans taken from a molecular layer before and after the deposition of a top metal layer [32]. The procedure applied is as follows: we first measured a XRR scan on a single C_{60} layer deposited on top Si/SiO_2 (Fig. 3b). Afterwards, we placed the very same sample back in the evaporation chamber and deposited on top 8-nm-thick Py layer. The XRR scan measured on the full bilayer after the metal deposition is shown in Fig. 3c.

The fit to the data shown in Fig. 3b (red line) provides us with values of the layer thickness (18.7 nm), roughness (1.4 nm) and density (1.6 g/cm^3). These values were obtained by using as starting parameters in the fitting procedure the nominal thickness given by a thickness monitor during the deposition (20 nm), the roughness obtained by AFM measurements (0.65 nm), and the C_{60} nominal density (1.6 g/cm^3). In the case of the fit to the XRR data of the C_{60}/Py bilayer (Fig. 3c, red line), the starting parameters for the C_{60} layer are the values provided by the fit of the uncovered layer, while for the Py we used the nominal thickness (8 nm) and the nominal density (8.72 g/cm^3). From the fit, we obtain for the C_{60} layer the same density (1.6 g/cm^3) and for the Py layer a density (8.8 g/cm^3) and a thickness (7.8 nm) in good agreement with the expected values. Interestingly, we find that the C_{60} thickness diminished from 18.7 nm down to 17.5 nm after the top metal deposition. We can assume that after the metal deposition on the fullerene, exactly at the C_{60}/Py interface, an ill-defined layer with a thickness of approximately 1–2 nm is formed. The thickness of this layer is extremely thin compared to the damage reported to other molecular layers after a metal deposition [6,29,30].

From the data presented above we prove that the C_{60}/Py system fulfills as well the second condition proposed above (thin intermixing layer, in the order of 1 nm) for making it a suitable metal–organic reference system for molecular spintronics.

From the above discussion, the 5-nm-thick C_{60} layer would seem to be the limiting case between a short-circuited and a resistive vertical device, because 5 nm is just above the sum between the fullerene layer roughness and the interfacial ill-defined layer. Indeed, this fact is confirmed by the electrical characterization of devices where the Py layer is used as a top electrode. We produced vertical spin valves with the same geometry of Fig. 1, employing a Co/AlO_x bottom electrode, and a Py top electrode [5].

The thickness of the Py layer was kept fixed to 20 nm, while different C_{60} layer thicknesses were employed in different devices. For the 3-nm-thick C_{60} layer, we measured a very low resistance area product ($RA < 10^{-4}\ \Omega/cm^2$), most probably due to pinholes in the C_{60} layer that short-circuit the device. This suggestion is supported by the fact that the thickness of the C_{60} is lower than the sum between the roughness and the ill-defined interfacial layer. On the contrary, for the 5-nm-thick C_{60} layer, the device was not short-circuited, as shown in Fig. 4a. The resistance area product in this device is $RA = 10^{-2}\ \Omega/cm^2$, 2 orders of magnitude higher than the 3-nm-thick C_{60} device. However, the device gets short-circuited when a rather low voltage is applied to it (0.2 V), probably due to the high current density. An 8-nm-thick C_{60} layer device is more resistive ($RA = 50\ \Omega/cm^2$) and more stable (up to

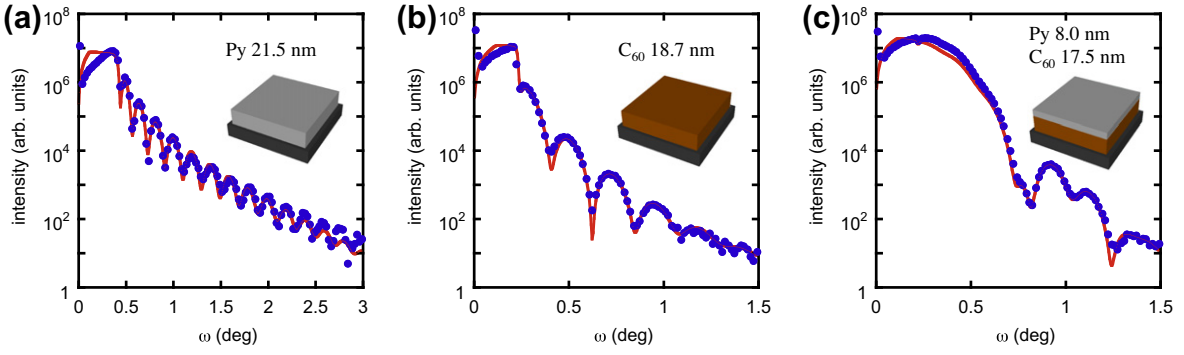

Fig. 3. X-ray reflectivity characterization of Py/C_{60} layers. Experimental data are shown as blue dots; the red line is the fit obtained by modeling the sample as (a) a single Py layer, (b) a single C_{60} layer, (c) a C_{60}/Py bilayer. The thicknesses displayed in the figure are those obtained from the fit. (For interpretation of the references to colour in this figure legend, the reader is referred to the web version of this article.)

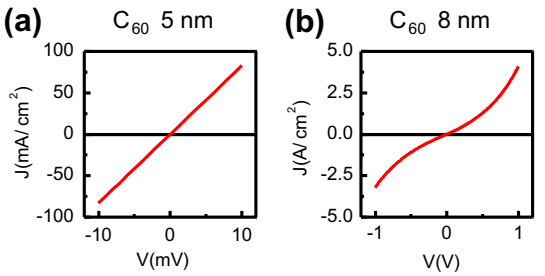

Fig. 4. Electrical characterization of vertical devices with variable-thickness C_{60} interlayers and Py top electrodes: current density vs applied voltage measured in a 5-nm-thick C_{60} layer (a) and a 8 nm-thick C_{60} layer (b).

1 V, Fig. 4b), confirming that 5 nm is around the limiting case between a short-circuited and a stable resistive device.

After having discussed the morphological and electrical properties of the Py and fullerene layers, we should turn now our attention to the magnetic properties of the metal film (see condition three above). It is clear that for producing optimum spin valves, the Py layer must conserve its magnetic properties unaltered when deposited either below or above a molecular layer.

It is generally expected that a molecular layer deposited on top of a FM metal would not affect dramatically the magnetic properties of the latter, although issues such as oxidation or a strong metal-molecular bonding have to be taken into account carefully [2,10]. For the opposite case, that is a FM layer on top a molecular one, it is not obvious to what extent the roughness of the molecular sub-layer affects the magnetic properties of the FM film [16–18]. In particular, the magnetic properties of the ill-defined layer at the interface need to be investigated.

The characterization of the magnetic properties of the different Py films has been done focusing on the two most representative parameters that define the magnetic hysteresis loop: the saturation magnetization (Ms) and the coercive field (Hc). For the first set of samples, in which C_{60} layers of different thicknesses cover a 5-nm-thick Py film, the Ms values are displayed with blue closed symbols and line in Fig. 5a. From the inspection of Fig. 5a we can conclude that the Ms values of the Py underlayer are not affected by the growth of the top C_{60} layer: Ms is constant within the error bars, irrespective of the amount of molecules deposited on top of the Py underlayer. Note that the first blue symbol corresponds to a C_{60} thickness equal to 0, so it represents the Ms of a Py film grown directly on Si/SiO_2.

The red open symbols and line in Fig. 5a refer to the Ms for the inverse set of samples in which different thicknesses of Py are deposited on top of the C_{60} underlayer. In this case, we find that the samples with Py thicknesses above 3 nm have again Ms constant within the error bar, with a value which is very close to the Ms measured for the previous samples. The 3-nm-thick Py layer (first red open symbol in Fig. 5a) shows a remarkably different behavior. It is ferromagnetic, because it displays a clear hysteresis loop, but its Ms value of 270 ± 20 emu/cm^3 corresponds to almost one third of the average Ms of the other samples. This considerable drop in Ms of this ultrathin layer can be explained considering that (1) the C_{60} surface peak-peak roughness is in the order of the Py thickness, so the layer may be not continuous (see above the discussion about the morphological properties of the Py/C_{60} system); (2) the thickness of the ill-defines layer between C_{60} and Py that we estimated in approximately 1–2 nm nm corresponds to almost one half of the Py layer thickness. In summary, the data displayed in Fig. 5a points to 5 nm as the lowest thickness of a Py overlayer to be continuous and with bulk magnetic properties.

In general, all our Py samples show a value for Ms of 720 ± 70 emu/cm^3, which is slightly lower than the reported saturation value for bulk Py (830 emu/cm^3) [33] and resulting closer to the Ms of pure Ni. Such a difference may be due to two concomitant factors. In the first place, the stoichiometry of the NiFe alloy is not conserved during the e-beam evaporation, with an effective lower Fe concentration in the film as observed by Energy Dispersive X-ray analysis (not shown). In the second place, the Fe could get oxidized to some minor extent during the deposition process, even if the pressure in the chamber during the metal deposition was around 10^{-7} mbar. In both cases the Ms would deviate from the standard Py saturation and move to a value closer to the pure Ni saturation magnetization (488 emu/cm^3) [33].

Additional hints about the magnetic properties of the different Py films in combination with C_{60} are provided by the values of the coercive field Hc, which gives us information regarding the relation between the external applied magnetic field and the energy required for reversing the magnetization direction.

In Fig. 5b, we show with blue and red symbols the Hc of the bilayers with the magnetic Py films placed as bottom or as top electrode, respectively. We must point out here that all our Py films show a weak uniaxial magnetic anisotropy, probably due to a small remnant field at the sample stage during the deposition. Therefore, in Fig. 5b we include only the Hc values measured along the direction of easy magnetization (easy-axis) for a consistent comparison between different samples. Fig. 5b shows that the C_{60} grown on top of the Py film has not any influence on its hysteresis loop. The coercive fields recorded are all in the range from 1.5 to 2 Oe, which are very close to the value obtained in the case of a plain Py film without any C_{60} above (first blue point in Fig. 5b). The average coercive field increases to 3.5 Oe for the Py films grown on top of C_{60}. This difference can be also visualized in Fig. 5c, which shows the hysteresis loop of a 5 nm Py layer placed as top and bottom electrode (blue and red curve, respectively). The significant difference in Hc is due to the intrinsic roughness of the underlying C_{60} layer (see above), which creates magnetic pinning sites (orange-peel like effect [34]) in the top Py film [16–18]. In any case, although the difference in the coercive field of the two cases is proportionally very large, its absolute value remains very small. In conclusion, the magnetic properties of the Py layer are not drastically affected by the C_{60} underneath.

Following the magnetic characterization performed in the Py/C_{60} system, we can now assure that such combina-

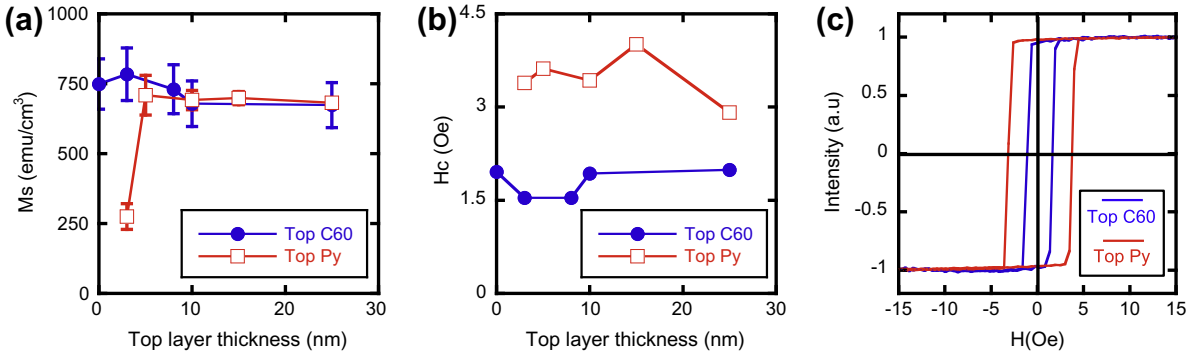

Fig. 5. Magnetic characterization of C_{60}-Py bilayers. Magnetization and coercive field are shown for two sets of samples: in the first set, Py layers of fixed thickness (5 nm) are covered by C_{60} layers with variable thickness; in the second set, C_{60} layers of fixed thickness (16 nm) are covered by Py layers with variable thickness. For the first sample set, Ms and Hc are plotted as a function of the thickness of the top C_{60} layer (blue closed data in (a) and (b), respectively). For the second set, Ms and Hc are plotted as a function of thickness of the top Py layer (red open data in a and b respectively). The main error source comes from the thickness of the FM layer, which we estimate in 0.5 nm. (c) Shows the hysteresis loop of a 5-nm-thick Py when it is placed below a 8 nm C_{60} film (blue closed circles) and above a 16-nm-thick C_{60} film (red open squares). (For interpretation of the references to colour in this figure legend, the reader is referred to the web version of this article.)

tion of materials fulfills as well the third condition for an ideal materials test system in molecular spintronics outlined above.

4. Conclusion

In this letter, we characterized structurally, electrically and magnetically C_{60}/Py bilayers combining different techniques (AFM, XRR, SQUID, MOKE) in order to test their suitability as a base system for molecular-based spintronics. We have highlighted three general constrains that any bilayer needs to fulfill for being used in vertical spintronic devices: (1) the films need to grow smoothly; (2) the molecular layer should be minimally damaged by the top metal deposition; (3) the magnetic properties of the ferromagnetic layer need to be preserved.

We found that the C_{60}/Py bilayers satisfy these three constrains: the layers grow with low surface roughness and the intermixing between Py and C_{60} layers is limited to 1–2 nm, so that a 5-nm-thick C_{60} layer can be contacted without pinholes. Finally, a Py layer as thin as 5 nm already displays good magnetic properties even when it is grown on the rough C_{60} surface.

We can, thus, conclude that the combination between C_{60} and Py provides a robust platform for spintronic application. In particular, we suggest that this system is ideal to study the effect of further modifications (of the morphology and/or of the energetic) of the metal–organic interface.

Acknowledgments

This work is supported by the by the European Union 7th Framework Programme (NMP3-SL-2011-263104-HINTS), by the Spanish Ministry of Science and Education under Project No. MAT2009-08494 and MAT2009-07980 as well as by the Basque Government through the ETORGAI Program, Project "Biodetect" No. ER-2010/00032, and Programs No. PI2009-17.

References

[1] V.A. Dediu, L.E. Hueso, I. Bergenti, C. Taliani, Nat. Mater. 8 (2009) 707.
[2] C. Barraud, P. Seneor, R. Mattana, S. Fusil, K. Bouzehouane, C. Deranlot, P. Graziosi, L. Hueso, I. Bergenti, V. Dediu, F. Petroff, A. Fert, Nat. Phys. 6 (2010) 615.
[3] T.S. Santos, J.S. Lee, P. Migdal, I.C. Lekshmi, B. Satpati, J.S. Moodera, Phys. Rev. Lett. 98 (2007) 016601.
[4] J.J.H.M. Schoonus, P.G.E. Lumens, W. Wagemans, J.T. Kohlhepp, P.A. Bobbert, H.J.M. Swagten, B. Koopmans, Phys. Rev. Lett. 103 (2009) 146601.
[5] M. Gobbi, F. Golmar, R. Llopis, F. Casanova, L.E. Hueso, Adv. Mat. 23 (2011) 1609.
[6] Z.H. Xiong, D. Wu, Z. Valy Vardeny, J. Shi, Nature 427 (2004) 821.
[7] V. Dediu, L.E. Hueso, I. Bergenti, A. Riminucci, F. Borgatti, P. Graziosi, C. Newby, F. Casoli, M.P. De Jong, C. Taliani, Y. Zhan, Phys. Rev. B 78 (2008) 115203.
[8] T.D. Nguyen, G. Hukic-Markosian, F. Wang, L. Wojcik, X. Li, E. Ehrenfreund, Z.V. Vardeny, Nat. Mater. 9 (2010) 345.
[9] L. Schulz, L. Nuccio, M. Willis, P. Desai, P. Shakya, T. Kreouzis, V.K. Malik, C. Bernhard, F.L. Pratt, N.A. Morley, A. Suter, G.J. Nieuwenhuys, T. Prokscha, E. Morenzoni, W.P. Gillin, A.J. Drew, Nat. Mater. 10 (2011) 252.
[10] S. Sanvito, Nat. Phys. 6 (2010) 562.
[11] M. Prezioso, A. Riminucci, I. Bergenti, P. Graziosi, D. Brunel, V.A. Dediu, Adv. Mater. 23 (2011) 1371.
[12] Y. Zhan, E. Holmström, R. Lizárraga, O. Eriksson, X. Liu, F. Li, E. Carlegrim, S. Stafström, M. Fahlman, Adv. Mater. 22 (2010) 1626.
[13] M. Cinchetti, K. Heimer, J.P. Wüstenberg, O. Andreyev, M. Bauer, S. Lach, C. Ziegler, Y. Gao, M. Aeschlimann, Nat. Mater. 8 (2008) 115.
[14] M. Barra, A. Cassinese, P. D'Angelo, L.E. Hueso, P. Graziosi, V. Dediu, Org. Elec. 9 (2008) 911.
[15] V.Yu. Aristov, O.V. Molodtsova, Yu.A. Ossipyan, B.P. Doyle, S. Nannarone, M. Knupfer, Org. Elec. 10 (2009) 8.
[16] Y. Chan, Y. Hung, C. Wang, Y. Lin, C. Chiu, Y. Lai, H. Chang, C. Lee, Y.J. Hsu, D.H. Wei, Phys. Rev. Lett. 104 (2010) 177204.
[17] A.A. Sidorenko, C. Pernechele, P. Lupo, M. Ghidini, M. Solzi, R. De Renzi, I. Bergenti, P. Graziosi, V. Dediu, L. Hueso, A.T. Hindmarch, Appl. Phys. Lett. 97 (2010) 162509.
[18] I. Bergenti, A. Riminucci, E. Arisi, M. Murgia, M. Cavallini, M. Solzi, F. Casoli, V. Dediu, J. Magn. Magn. Mater. 316 (2007) e987.
[19] T.L.A. Tran, P.K.J. Wong, M.P. de Jong, W.G. van der Wiel, Y.Q. Zhan, M. Fahlman, Appl. Phys. Lett. 98 (2011) 222505.
[20] K.V. Raman, J. Chang, J.S. Moodera, Org. Elec. 12 (2011) 1275.
[21] J.S. Jiang, J.E. Pearson, S.D. Bader, Phys. Rev. Lett. 106 (2011) 156807.
[22] F.J. Jedema, A.T. Filip, B.J. van Wees, Nature 410 (2001) 345.
[23] J.S. Moodera, L.R. Kinder, T.M. Wong, R. Meservey, Phys. Rev. Lett. 74 (1995) 3273.
[24] S. Miwa, M. Shiraishi, S. Tanabe, M. Mizuguchi, T. Shinjo, Y. Suzuki, Phys. Rev. B 76 (2007) 214414.
[25] F.Wang, Z. V. Vardeny, Synth. Met. 160 (2010) 210.

[26] P. Vavassori, Appl. Phys. Lett. 77 (2000) 1605.
[27] H. Haick, O. Niitsoo, J. Ghabboun, D. Cahen, J. Phys. Chem. C 111 (2007) 2318.
[28] H. Haick, J. Ghabboun, D. Cahen, Appl. Phys. Lett. 86 (2005) 042113.
[29] A.C. Durr, F. Schreiber, M. Kelsch, H.D. Carstanjen, H. Dosch, Adv. Mat. 14 (2002) 961.
[30] B. de Boer, M.M. Frank, Y.J. Chabal, W. Jiang, E. Garfunkel, Z. Bao, Langmuir 20 (2004) 1539.
[31] O. Amelines-Sarria, P.C. dos Santos Claro, P.L. Schilardi, B. Blum, A. Rubert, G. Benitez, V.A. Basiuk, A. González Orive, A. Hernández Creus, C. Díaz, R.C. Salvarezza, Org. Elec. 12 (2011) 1483.
[32] C.R. Hansen, T.J. Sørensen, M. Glyvradal, J. Larsen, S.H. Eisenhardt, T. Bjørnholm, M.M. Nielsen, R. Feidenhans'l, B.W. Laursen, NanoLett. 9 (2009) 1052.
[33] Coey, Magnetism and magnetic materials, Cambridge University press, Cambridge, 2009.
[34] L. Néel, C.R. Acad, Sci., Ser. A 255 (1962) 1676.